

Large Variations in One-Bond $^{13}\text{C}^\alpha\text{--}^{13}\text{C}^\beta$ J Couplings in Polypeptides Correlate with Backbone Conformation

Gabriel Cornilescu,[†] Ad Bax,^{*,†} and David A. Case^{*,‡}

Contribution from the Laboratory of Chemical Physics, National Institute of Diabetes and Digestive and Kidney Diseases, National Institutes of Health, Bethesda, Maryland 20892, and Department of Molecular Biology, The Scripps Research Institute, La Jolla, California 92037

Received October 7, 1999. Revised Manuscript Received December 14, 1999

Abstract: One-bond $^1J_{\text{CaC}\beta}$ scalar couplings, measured in the protein ubiquitin, exhibit a strong dependence on the local backbone conformation. Empirically, the deviation from the $^1J_{\text{CaC}\beta}$ value measured in the corresponding free amino acid, can be expressed as $\Delta^1J_{\text{CaC}\beta} = 1.3 + 0.6 \cos(\psi - 61^\circ) + 2.2 \cos[2(\psi - 61^\circ)] - 0.9 \cos[2(\phi + 20^\circ)] \pm 0.5$ Hz, where ϕ and ψ are the intraresidue polypeptide backbone torsion angles obtained from ubiquitin's X-ray structure. The relation between $^1J_{\text{CaC}\beta}$ and backbone torsion angles is confirmed by density functional theory (DFT) calculations on the peptide analogue Ace-Ala-NMe.

Introduction

Structure determination of bacterially expressed proteins commonly relies on the use of uniform isotopic enrichment with ^{13}C and ^{15}N .^{1–4} This has made it possible to measure ^{13}C shifts and many types of homo- and heteronuclear J couplings in such proteins and to establish extensive and highly accurate empirical correlations between these NMR parameters and the local conformation of the polypeptide.^{5–11}

This study focuses on the variation in one-bond $^1J_{\text{CaC}\beta}$ couplings observed in a small protein and its dependence on local geometry. It has long been recognized that $^1J_{\text{CC}}$ couplings are dominated by the Fermi-contact contribution and can be influenced by steric effects and interaction with lone-electron pairs.^{12–15} Nevertheless, relatively few data are available which correlate $^1J_{\text{CC}}$ with local structure in an unambiguous manner, because such comparisons usually are influenced both by steric and substituent effects. In proteins, all $^{13}\text{C}^\alpha$ sites carry very

similar substituents (except glycine), and $^{13}\text{C}^\beta$ substituents fall in a small number of groups. Therefore, they offer a unique opportunity to study the effect of conformation on $^1J_{\text{CC}}$.

A previous experimental study of $^1J_{\text{CaH}\alpha}$ showed a strong correlation between this coupling and the backbone torsion angles ϕ and ψ , with the largest values observed in α -helices and the smallest ones for residues in tight turns with positive ϕ angles.^{16,17} Here, we show that the opposite trend is observed for $^1J_{\text{CaC}\beta}$. Recent advances in computational chemistry now make it possible to calculate quite accurate predictions of NMR parameters such as J couplings.^{18–25} We include results from density functional theory (DFT) calculations, which confirm the strong dependence of $^1J_{\text{CaC}\beta}$ on local geometry. The substantial variation observed for $^1J_{\text{CC}}$ in proteins is also of consequence for experiments such as CCH- and HCCH-COSY and TOCSY experiments,^{26–28} where these couplings are used to transfer magnetization for resonance assignment purposes.

Experimental Section

All measurements were carried out on a Bruker DMX-600 spectrometer, equipped with a pulsed field gradient triple resonance probehead. $^1J_{\text{CaC}\beta}$ values in free amino acids were measured for Ala, Asp, Ile, Leu, Lys, Pro, Ser, Thr, Tyr, and Val, using a 2D $^1\text{H}\text{--}^{13}\text{C}$ HSQC experiment with a long (120 ms) t_1 acquisition time. All

[†] National Institute of Diabetes and Digestive and Kidney Diseases, National Institutes of Health.

[‡] The Scripps Research Institute.

(1) Edison, A. S.; Abildgaard, F.; Westler, W. M.; Mooberry, E. S.; Markley, J. L. *Methods Enzymol.* **1994**, *239*, 3–79.

(2) Gronenborn, A. M.; Clore, G. M. *Crit. Rev. Biochem. Mol.* **1995**, *30*, 351–385.

(3) Clore, G. M.; Gronenborn, A. M. *Nat. Struct. Biol.* **1997**, *4*, 849–853.

(4) Dötsch, V.; Wagner, G. *Curr. Opin. Struct. Biol.* **1998**, *8*, 619–623.

(5) DeMarco, A.; Llinas, M.; Wüthrich, K. *Biopolymers* **1978**, *17*, 2727–2742.

(6) Pardi, A.; Wagner, G.; Wüthrich, K. *Eur. J. Biochem.* **1983**, *137*, 445–454.

(7) Spera, S.; Bax, A. *J. Am. Chem. Soc.* **1991**, *113*, 5491–5492.

(8) Wishart, D. S.; Sykes, B. D. *J. Biomol. NMR* **1994**, *4*, 171–180.

(9) Wang A. C.; Bax A. *J. Am. Chem. Soc.* **1996**, *118*, 2483–2494.

(10) Hu J.-S.; Bax A. *J. Am. Chem. Soc.* **1997**, *119*, 6360–6368.

(11) Schmidt, J. M.; Blumel, M.; Lohr, F.; Rüterjans, H. *J. Biomol. NMR* **1999**, *14*, 1–12.

(12) Lynden-Bell, R. M.; Sheppard, N. *Proc. R. Soc.* **1962**, *269A*, 385–403.

(13) Barna, J. C. J.; Robinson, J. T. *Tetrahedron Lett.* **1979**, *16*, 1459–1462.

(14) Summerhays, K. D.; Maciel, G. E. *J. Am. Chem. Soc.* **1972**, *94*, 8348–8351.

(15) Krivdin, L. B.; Kalabin, G. A. *Prog. Nucl. Magn. Reson. Spectrosc.* **1989**, *21*, 293–448.

(16) Mierke, D. F.; Grdadolnik, S. G.; Kessler, H. *J. Am. Chem. Soc.* **1992**, *114*, 8283–8284.

(17) Vuister, G. W.; Delaglio, F.; Bax A. *J. Am. Chem. Soc.* **1992**, *114*, 9674–9675.

(18) Onak, T.; Jaallas, J.; Barfield, M. *J. Am. Chem. Soc.* **1999**, *121*, 2850–2856.

(19) Dingley, A. J.; Masse, J. E.; Peterson, R. D.; Barfield, M.; Feigon, J.; Grzesiek, S. *J. Am. Chem. Soc.* **1999**, *121*, 6019–6027.

(20) Barfield, M.; Smith, W. B. *J. Am. Chem. Soc.* **1992**, *114*, 1574–1581.

(21) Case, D. A.; Dyson, H. J.; Wright, P. E. *Methods Enzymol.* **1994**, *239*, 392–416.

(22) Barfield, M. In *Encyclopedia of Nuclear Magnetic Resonance*; Grant, D. M., Harris, R. K., Eds; Wiley: London, 1996; pp 2520–2532.

(23) Malkina, O. L.; Salahub, D. R.; Malkin, V. G. *J. Chem. Phys.* **1996**, *105*, 8793–8800.

(24) Helgaker, T.; Jaszunski, M.; Ruud, K. *Chem. Rev.* **1999**, *99*, 293–352.

(25) Cloran, F.; Carmichael, I.; Serianni, A. S. *J. Phys. Chem. A* **1999**, *103*, 3783–3795.

measurements were done at pH 6.8 and at concentrations ranging from 0.5 to 30 mM, depending on quantities available.

$^1J_{\text{CaC}\beta}$ values in the small protein ubiquitin (76 residues) were measured using a sample containing 1.3 mM $^{13}\text{C}/^{15}\text{N}$ -ubiquitin (VLI Research, Malvern, PA) in 95% H_2O , 5% D_2O , pH 6.5, 10 mM phosphate buffer, in a 250 μL Shigemi microcell. Couplings were measured from a 3D HN(CO)CA experiment,²⁹ with a relatively long acquisition time of 60 ms in the $^{13}\text{C}^\alpha$ dimension. The spectrum was acquired as a $200^* (t_1, ^{13}\text{C}) \times 84^* (t_2, ^{15}\text{N}) \times 512^* (t_3, ^1\text{H})$ data matrix, with 8 scans per hypercomplex (t_1, t_2) pair. The total measuring time was 38 h.

Spectra were apodized with 60° -shifted sine bell windows in all dimensions, and data were zero-filled prior to Fourier transformation to yield a digital resolution of 3.3 Hz ($^{13}\text{C}^\alpha$), 9.3 Hz (^{15}N) and 8.3 Hz (^1H). Data were processed and peak-picked using the NMRPipe software package.³⁰

DFT calculations were carried out on conformers of an alanine dipeptide analogue, Ace-Ala-NMe, where the ϕ and ψ backbone angles were constrained to values on a 30° grid, with the remaining degrees of freedom optimized using Hartree–Fock theory and a 6-31G basis set. Only fairly low-energy ϕ, ψ pairs were considered, as documented earlier.³¹ Indirect spin–spin coupling constants were determined using the deMon program.^{23,32,33} We used the IGLO-III basis set of Kutzelnigg and co-workers;³⁴ this is a relatively large basis set, with 11 s-type and 7 p-type Gaussians on first row atoms (contracted to 7s/6p) along with two uncontracted polarization functions. All calculations used the Perdew–Wang-91 (PW91) exchange functional with the Perdew correlation functional.^{35,36} The diamagnetic spin–orbit (DSO), paramagnetic spin–orbit (PSO), and Fermi contact (FC) contributions are computed with this approach. For the Fermi term, a finite perturbation approach is used, so that a separate calculation is needed for each nucleus, although such a calculation then gives couplings to all other nuclei in the molecule. The DSO and PSO terms are small and partially cancel, so that the net coupling is dominated by the FC term. For example, for the alanine dipeptide with $(\phi, \psi) = (-60, -60)$, the FC, DSO, and PSO contributions to $^1J_{\text{CaC}\beta}$ are 29.3, -0.6 , and 0.3 Hz, respectively. For the alanine dipeptide, each calculation takes about 2.5 h of CPU time on a single processor of a 450 MHz Cray T3E. Two such calculations were carried out (with the perturbation applied at the H^α and C^β positions) for each of 56 Hartree–Fock optimized structures.

Results and Discussion

Empirical Correlation between $^1J_{\text{CaC}\beta}$ and Torsion Angles. $^1J_{\text{CaC}\beta}$ coupling constants measured for free amino acids were found to be similar to those in the literature.^{37–39} Here,

(26) Fesik, S. W.; Gampe, R. T.; Zuiderweg E. R. *J. Am. Chem. Soc.* **1989**, *111*, 770–772.

(27) Kay, L. E.; Ikura, M.; Bax, A. *J. Am. Chem. Soc.* **1990**, *112*, 888–889.

(28) Clore, G. M.; Kay, L. E.; Bax, A.; Gronenborn, A. M. *Biochemistry* **1991**, *30*, 12–18.

(29) Bax, A.; Ikura, M. *J. Biomol. NMR* **1991**, *1*, 99–104.

(30) Delaglio, F.; Grzesiek, S.; Vuister, G. W.; Zhu, G.; Pfeifer, J.; Bax, A. *J. Biomol. NMR* **1995**, *6*, 277–293.

(31) Sitkoff, D.; Case, D. A., *J. Am. Chem. Soc.* **1997**, *119*, 12262–12273.

(32) Malkin, V. G.; Malkina, O. L.; Salahub, D. R. *Chem. Phys. Lett.* **1994**, *221*, 91–99.

(33) Malkin, V. G.; Malkina, O. L.; Eriksson, L. A.; Salahub, D. R. In *Modern Density Functional Theory: A Tool for Chemistry*; Seminario, J. M., Politzer, P., Eds.; Elsevier: Leiden, 1995; pp 273–347.

(34) Kutzelnigg, W.; Fleischer, U.; Schindler, M. In *NMR, Basic Principles and Progress*; Diehl, P., Fluck, E., Günther, H., Kosfeld, R., Seelig, J., Eds.; Springer: Berlin, 1990; Vol. 23, pp 167–262.

(35) Perdew, J. P.; Wang, Y. *Phys. Rev. B* **1992**, *45*, 13244–13249.

(36) Perdew, J. P. *Phys. Rev. B* **1986**, *33*, 8822–8824.

(37) Tran-Dinh, S.; Femandjian, S.; Sala, E.; Mermet-Bouvier, R.; Fromageot, P. *J. Am. Chem. Soc.* **1975**, *97*, 1267–1269.

(38) London, R. E.; Walker, T. E.; Kolman, V. H.; Matwiyoff, N. A. *J. Am. Chem. Soc.* **1978**, *100*, 3723–3729.

(39) Tran-Dinh, S.; Femandjian, S.; Sala, E.; Mermet-Bouvier, R.; Cohen, M.; Fromageot, P. *J. Am. Chem. Soc.* **1974**, *96*, 1484–1493.

Table 1. Values Used for $^1J_{\text{CaC}\beta}$ (Hz) at Neutral pH in Free Amino Acids

residue type	$^1J_{\text{CaC}\beta}$
Ala	35.0 ^{a,d}
Arg	34.3 ^e
Asn	36.4 ^f
Asp	36.4 ^{a,b,c}
Gln	34.3 ^c
Glu	34.3 ^c
His	33.6 ^g
Ile	33.7 ^{a,d}
Leu	34.3 ^{a,d}
Lys	34.3 ^{a,b}
Phe	33.6 ^g
Pro	33.0 ^a
Ser	37.4 ^a
Thr	37.3 ^a
Tyr	33.6 ^a
Val	33.6 ^{a,c}

^a This study. ^b From ref 37. ^c From ref 38. ^d From ref 39. ^e Assumed to be the same as Lys. ^f Assumed to be the same as Asp. ^g Assumed to be the same as Tyr.

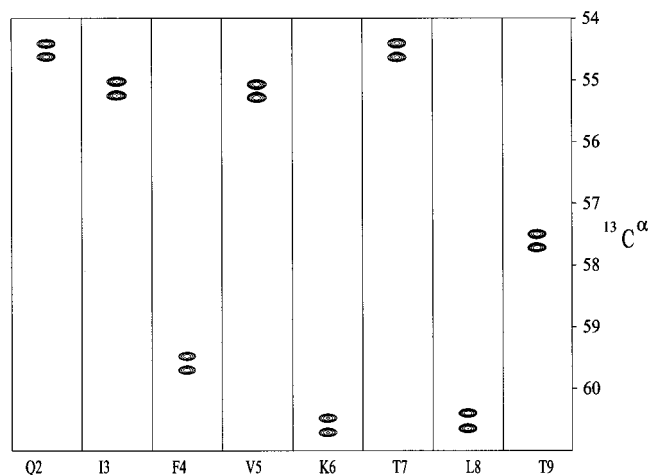


Figure 1. Strips taken from the 600 MHz 3D HN(CO)CA spectrum of $^{13}\text{C}/^{15}\text{N}$ ubiquitin, showing the correlations between amides of residue 2–10 and the $^{13}\text{C}^\alpha$ of the preceding residue. The splitting in the $^{13}\text{C}^\alpha$ dimension corresponds to $^1J_{\text{CaC}\beta}$.

we assume that the values measured at neutral pH in free amino acids correspond to the “random coil” value for $^1J_{\text{CaC}\beta}$. Values measured in this study, together with those available from the literature, are listed in Table 1. As can be seen from this table, substantial variation exists in the free amino acid values, ranging from 33.0 Hz for Pro, to 36.4, 37.3, and 37.4 Hz for Asp, Thr, and Ser, which carry electronegative substituents at C^β .

Figure 1 shows several small cross sections taken from the HN(CO)CA spectrum, displaying the quality of the protein data used in this study. Repeating the measurement yielded a pairwise root-mean-square-difference (rmsd) of 0.1 Hz, indicating a random uncertainty of 0.05 Hz in the averaged $^1J_{\text{CaC}\beta}$ values, obtained from the two data sets. Measured $^1J_{\text{CaC}\beta}$ values are presented in the Supporting Information.

Inspection of the $^1J_{\text{CaC}\beta}$ values shows a distinct effect of secondary structure on the deviation, $\Delta^1J_{\text{CaC}\beta}$, of the measured coupling from that in the free amino acid. The average $^1J_{\text{CaC}\beta}$ value in ubiquitin’s α -helix is 33.7 Hz, the average value in β sheet is 35.0 Hz, and their respective $\Delta^1J_{\text{CaC}\beta}$ values are -0.9 ± 0.5 and $+0.4 \pm 0.7$ Hz. The largest $\Delta^1J_{\text{CaC}\beta}$ values (up to 4.9 Hz) are seen for residues with positive ϕ angles (Supporting Information).

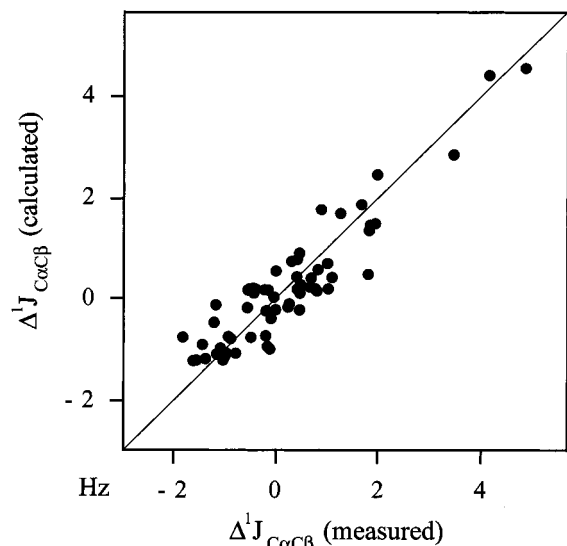


Figure 2. Plot of $\Delta^1J_{CaC\beta}$ values predicted on the basis of empirical eq 1 and crystallographic ϕ and ψ angles, versus experimentally measured $\Delta^1J_{CaC\beta}$ values. The correlation coefficient, R , equals 0.92.

Ubiquitin's crystal structure⁴⁰ is in excellent agreement with the solution NMR structure, except for residues 72–76, which are not ordered in solution.^{41,42} Fully analogous to the earlier study of $^1J_{CaH\alpha}$,^{17,43} an empirical correlation between $\Delta^1J_{CaC\beta}$ and the backbone torsion angles, ϕ and ψ , obtained from the crystal structure can be generated, yielding

$$\Delta^1J_{CaC\beta} = 0.6 \cos(\psi - 61^\circ) + 2.2 \cos[2(\psi - 61^\circ)] - 0.9 \cos[2(\phi + 20^\circ)] + 1.3 \text{ Hz} \quad (1)$$

where the flexible C-terminal tail has not been included in the fit. Adding an additional term, $A \cos(\phi + B)$, to this equation does not yield a statistically meaningful improvement in the quality of the fit. Figure 2 displays the correlation between values predicted by eq 1, and experimental values. The correlation coefficient, R , equals 0.92.

Theoretical Calculations. The basic DFT results for $^1J_{CaC\beta}$ are shown in Figure 3; for comparison, results for the more commonly studied $^1J_{CaH\alpha}$ coupling are shown in Figure 4. The greatest dependence is on the ψ backbone angle, with $^1J_{CaC\beta}$ showing large values near $\psi = 60^\circ$, whereas $^1J_{CaH\alpha}$ is large near $\psi = -60^\circ$. This implies that $^1J_{CaH\alpha}$ will tend to be larger in helical regions (where ψ is near -60°) than in extended or sheet structures (where ψ is positive). Roughly the opposite should hold for $^1J_{CaC\beta}$, which is predicted to be smallest for helical regions near $\psi = -60^\circ$, larger for sheets (where ψ is most often in the 90 – 150° range), and largest for right-handed helices (with ϕ and ψ near $+60^\circ$). All of these trends are in full agreement with measurements reported above for $^1J_{CaC\beta}$ and earlier for $^1J_{CaH\alpha}$. The predicted spread in coupling constants, about 6 Hz for $^1J_{CaC\beta}$ and about 18 Hz for $^1J_{CaH\alpha}$, is also in accord with observed values.

Figure 3 also shows the results of the empirical fit of eq 1 for $\phi = 180^\circ$ as a dashed line. It is clear that the basic dependence on ψ is very similar to the DFT results in the range

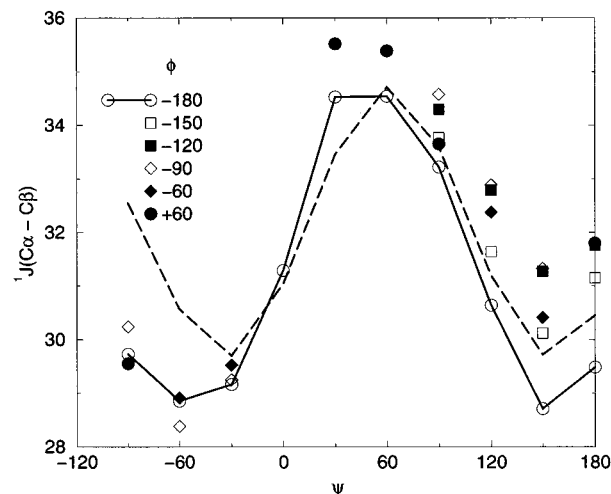


Figure 3. DFT results for $^1J_{CaC\beta}$, in Hz. The solid line for $\phi = 180^\circ$ is drawn to guide the eye. The dashed line shows the empirically derived eq 1, also using $\phi = 180^\circ$ after adding a random-coil $^1J_{CaC\beta}$ value of 31.3 Hz. Note that this random-coil $^1J_{CaC\beta}$ value is 3 Hz smaller than the experimental random coil value (see text).

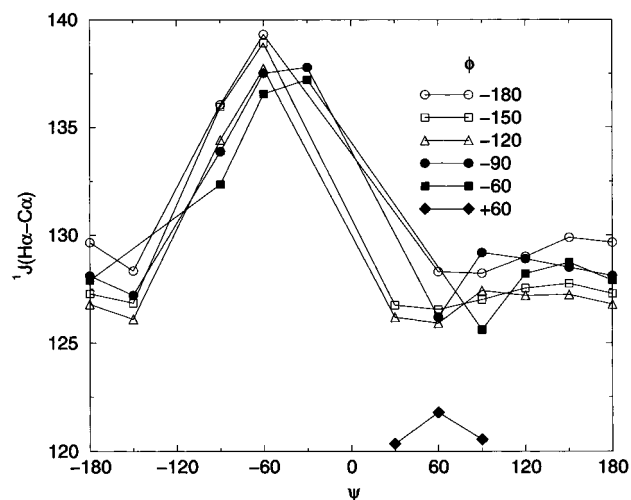


Figure 4. DFT results for $^1J_{CaH\alpha}$, in Hz.

$-60^\circ < \psi < 180^\circ$. Equation 1 predicts a second maximum near $\psi = -120^\circ$, but this is in a high-energy region that is rarely found in proteins and was not sampled in the quantum results or in the experimental data. The discrepancy in Figure 3 between the theoretical and empirical $^1J_{CaC\beta}$ values in the vicinity of $\psi = -90^\circ$ therefore is likely caused by the use of eq 1 outside the region where it was calibrated and suggests that care should be exercised when interpreting data for residues with ψ angles in this region.

The calculated dependence upon ψ can most easily be rationalized in terms of an interaction that increases the coupling when the $C^\alpha-C^\beta$ or $C^\alpha-H^\alpha$ bond is eclipsed by the adjacent carbonyl bond, that is, when the $C^\alpha-C^\beta-C-O$ or $H^\alpha-C^\alpha-C-O$ torsion angle is near zero. Figure 5 shows four typical conformers for the alanine dipeptide analogue. When ψ is near -60° (as in the α -helical conformation, shown at the upper left), the $C^\alpha-H^\alpha$ bond is eclipsed with the carbonyl bond in the same residue. Similarly, when ψ is near $+60^\circ$, as in the two conformations at the right), it is the $C^\alpha-C^\beta$ bond that is eclipsed to the carbonyl bond. While other geometric parameters must contribute to some extent (so that for a given ψ angle the computed couplings vary by 1–2 Hz), the configuration of the adjacent $C=O$ bond appears to be the single most important

(40) Vijay-Kumar, S.; Bugg, C. E.; Cook, W. J. *J. Mol. Biol.* **1987**, *194*, 531–544.

(41) Schneider, D. M.; Dellwo, M. J.; Wand, A. J. *Biochemistry* **1992**, *31*, 3645–3652.

(42) Tjandra, N.; Feller, S. E.; Pastor, R. W.; Bax, A. *J. Am. Chem. Soc.* **1995**, *117*, 12562–12566.

(43) Vuister, G. W.; Delaglio, F.; Bax, A. *J. Biomol. NMR* **1993**, *3*, 67–80.

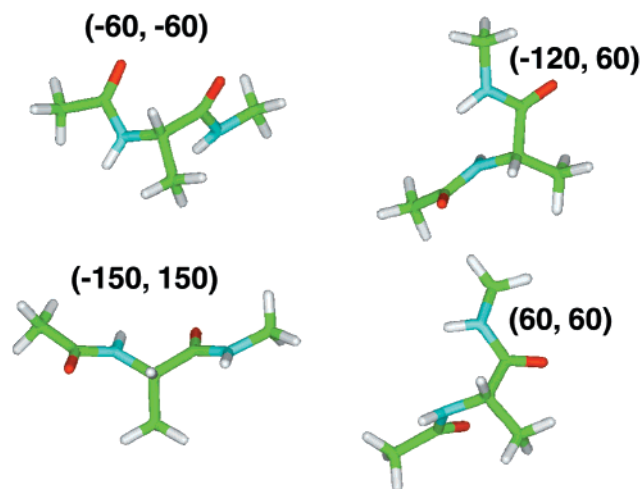


Figure 5. Four typical conformations of the alanine dipeptide analogue. Upper left: left-handed α -helix; lower left: β -sheet; upper right: polyproline; lower right: right-handed α -helix. The backbone torsion angles (ϕ, ψ) for the center Ala residue are marked in brackets.

Table 2. Calculated Values for Valine and Leucine Dipeptides

	ϕ	ψ	$^1J_{\text{CaC}\beta}$	$^1J_{\text{CaHa}}$	
Ala	-60	-60	28.9	136.6	
Val			28.7	134.2	g^+
			28.5	135.1	g^-
			28.5	135.9	t
Leu			28.6	136.6	g^+
			28.3	133.9	g^-
			28.3	137.1	t
Ala	-120	120	32.8	127.2	
Val			31.8	125.5	g^+
			31.8	125.6	g^-
			32.3	127.8	t
Leu			32.8	128.1	g^+
			31.5	125.3	g^-
			32.3	128.2	t

^a Values in Hz. g^+ , g^- , and t refer to χ_1 angles near 60°, -60°, and 180°, respectively. For leucine, χ_2 was near 180°.

feature influencing the computed values; this is consistent with ψ being a more important variable than ϕ for these couplings.

The chemical nature and conformation of the amino acid side chain is expected to have some influence on spin-spin couplings, and may be involved in the residual scatter from the empirical or theoretical curves described above. A full investigation of this would require much more experimental and theoretical data. Some initial computational indications are given in Table 2, which shows results for the valine and leucine dipeptides in helical and sheetlike conformations, for several values of the side chain torsion angle χ_1 . The basic trends described above for the alanine dipeptide are clearly evident for the other two side chains: The $\text{C}^\beta\text{--C}^\alpha$ coupling constant is nearly 4 Hz higher in the sheet than in the helical conformation, whereas the $\text{C}^\alpha\text{--H}^\alpha$ coupling is about 9 Hz larger in the helical

conformation. Variation due to the χ angle is 0.5–1 Hz for the $\text{C}^\beta\text{--C}^\alpha$ coupling and 2–3 Hz for $\text{C}^\alpha\text{--H}^\alpha$. Hence, it is likely that a precise interpretation of these couplings must consider the side chain in more detail than we have done here; nevertheless, the principal dependence on the ψ backbone angle appears to be reasonably independent of the side chain identity or position.

Concluding Remarks

Although the calculated dependence on conformation for $^1J_{\text{CaC}\beta}$ and $^1J_{\text{CaHa}}$ is in good accord with experiment, it should be noted that the absolute values of the calculated couplings are too small, by about 3 Hz for $^1J_{\text{CaC}\beta}$ and 10 Hz for $^1J_{\text{CaHa}}$. This may be due to a variety of effects, including the use of Hartree–Fock optimized geometries, neglect of vibrational averaging and environmental effects, and deficiencies in the basis set or density functionals. The present results are much more accurate than those of a previous study using the Hartree–Fock method and a 3-21G basis set⁴⁴ (where computed $^1J_{\text{CaHa}}$ values needed to be scaled by a factor of 2.5 to be in accord with experiment), but there is still room for improvement in our understanding of the theoretical origins of these couplings.

The scatter observed in Figure 2 (± 0.5 Hz) is considerably larger than the uncertainty in the experimental measurement. This indicates that factors other than ϕ and ψ also have a nonnegligible influence on $^1J_{\text{CaC}\beta}$. The same was previously noted for $^1J_{\text{CaHa}}$.^{17,43} Remarkably, the values for $\Delta^1J_{\text{CaC}\beta}^{\text{pred}} - \Delta^1J_{\text{CaC}\beta}^{\text{meas}}$ do not show a strong correlation with those for $\Delta^1J_{\text{CaHa}}^{\text{pred}} - \Delta^1J_{\text{CaHa}}^{\text{meas}}$ (data not shown), where the superscripts “pred” and “meas” refer to the values predicted on the basis of the empirical equations and the measured values, respectively. This indicates that these “other factors”, which may include χ_1 and χ_2 side chain torsion angles and the $\text{N--C}^\alpha\text{--C}'$ bond angle, are of very different relative importance for $^1J_{\text{CaHa}}$ and $^1J_{\text{CaC}\beta}$ couplings. Measurement of $^1J_{\text{CaC}\beta}$ is expected to become more common in small proteins as this value is needed for accurate measurement of the dipolar interaction between $^{13}\text{C}^\alpha$ and $^{13}\text{C}^\beta$, $^1\text{D}_{\text{CaC}\beta}$, when such proteins are aligned with the magnetic field in a dilute liquid crystalline phase. Together with $^1\text{D}_{\text{CaC}'}$ and $^1\text{D}_{\text{CaHa}}$, $^1\text{D}_{\text{CaC}\beta}$ provides unique information to define the orientation of a C^α site relative to the frame of a nonaxially symmetric molecular alignment tensor.

Acknowledgment. We thank Dennis A. Torchia and Cambridge Isotope Labs for gifts of ^{13}C -enriched amino acids. Work by G.C. is in partial fulfillment for the Ph.D. degree at the University of Maryland, College Park, MD. This work was supported by the AIDS Targeted Anti-Viral Program of the Office of the Director of the National Institutes of Health (to A.B.) and by NIH Grant GM48815 (to D.A.C.).

Supporting Information Available: One table containing the experimental $^1J_{\text{CaC}\beta}$ couplings in ubiquitin and one table containing the $\Delta^1J_{\text{CaC}\beta}$ values and backbone torsion angles in human ubiquitin (PDF). This material is available free of charge via the Internet at <http://pubs.acs.org>.

(44) Edison, A. S.; Markley, J. L.; Weinhold, F. J. *Biomol. NMR* **1994**, *4*, 519–542.